

Received: December 2023 Accepted: January 2024

DOI: <https://doi.org/10.58262/ks.v12i2.218>

## Application of Geomatics Technology to Study the Snow Cover in Amadiya District Using Satellite Image (Landsat-8)”

Noura Zayed Aati<sup>1</sup>, Ahmad Majid Abbas<sup>2</sup>, Eman Shihab Hassoun<sup>3</sup>, Salam Saud Hussein<sup>4</sup>, Ruqaya M. Amin<sup>5</sup>

### Abstract

*The aim of the research is to uncover the snow cover, relying on Landsat-8 satellite data through the utilization of the Normalized Difference Snow Index (NDSI) to detect the thickness, extent, and distribution of the snow layer covering the area on February 18, 2023. At the administrative unit level in the district, the research found that the distribution of snow cover in the Kani Masi district is the highest at 33.29%, while the center of the Al-Amadiyah district has the lowest distribution of snow cover at 2.57%. In terms of snow cover area, the Kani Masi sub-district ranked first at 86.02%, while the Bama Rani sub-district ranked last at 29.66%. The thickness of the snow cover (1 meter) constituted the largest percentage of the study area at 56.34%, while the thinnest thickness (0.04 cm) accounted for 7.98% of the total area.*

**Keywords:** Snow Cover, NDSI (Normalized Difference Snow Index), Geomatics, Landsat 8.

### 1. Introduction

Remote sensing has become one of the most advanced methods for measuring seasonal snow cover since its emergence in the mid-1960s. Data collected from visible, near-infrared, infrared, and microwave parts of the electromagnetic spectrum have proven useful for measuring various snow characteristics. Remote sensing provides the necessary data for studying different phenomena, especially those related to natural occurrences.

It serves as a powerful alternative for obtaining environmental data worldwide over time, with unprecedented temporal, spatial, and spectral accuracy. Snow, formed when temperatures drop below freezing, reflects radiation more than most materials and plays a crucial role in climate regulation. It provides surface and groundwater through melting for drinking purposes, irrigation, soil moisture, and reduces the risk of fires. Snow cover has a significant impact on surface radiation distribution, energy balances, and hydrology. The research addresses the problem of detecting and representing snow cover in a perceptible map format using digital processing in remote sensing and geographic information systems (GIS) environments.

This enhances the hypothesis that efficient digital maps of snow cover can be designed based on satellite data processing within the GIS environment. These maps contribute to extracting the area and depth of snow cover based on spectral indicators and clues, supporting decision-

<sup>1</sup> Aliraqia University, College of Arts, Department of Geography, Iraq. Email: noora.al-jizaniyah@aliraqia.edu.iq

<sup>2</sup> Aliraqia University, College of Arts, Department of Geography, Iraq. Email: ahmed.al-gburi@aliraqia.edu.iq

<sup>3</sup> Aliraqia University, College of Arts, Department of Geography, Iraq. Email: iman.al-ghrairi@aliraqia.edu.iq

<sup>4</sup> University of Tikrit, College of Education for Women, Department of Geography, Iraq. Email: salam.s@tu.edu.iq

<sup>5</sup> Aliraqia University, College of Arts, Department of Geography, Iraq. Email: ruqaya.mohamed@aliraqia.edu.iq

makers in solving environmental problems. Detection of snow layer type, including depth, using the Normalized Difference Snow Index (NDSI), as well as identifying the extent of snow cover and determining its distribution in the study area as of February 18, 2023, are among the research's primary objectives.

## 2. The Geographic Location of the Study Area

The geographic location of the study area: The boundaries of the study area are within the Al-Amadiyah district in Dohuk Governorate, Iraq. Geographically, it lies between longitudes ( $^{\circ}04.01^{\circ}43$ ) and ( $^{\circ}17.06^{\circ}44$ ) east and latitudes ( $^{\circ}16.50^{\circ}36$ ) and ( $^{\circ}21.30^{\circ}37$ ) north. It is bordered to the north by Turkey, to the south by the districts of Aqrah, Sheikhan, and the center of Dohuk district, to the east by the district of Merga Surr, and to the west by the district of Zakho, as shown in Figure (1). The area of the district is 2775.21 square kilometers, and it includes six sub-districts (Al-Amadiyah, Bamarni, Barwari, Kani Masi, Sarsink, and Nerwa Rakan). The elevation varies from 480 to 2559 meters above sea level.

**Table (1):** Tools, Methods, and Software Used.

Source	Year	Scale	Tool Used
Ministry of Industry and Minerals, General Authority for Survey and Mineral Investigation	2000	1:250000	Geological Map
Ministry of Water Resources, General Authority for Survey	2000	1:100000	Topographic Map
<a href="https://www.usgs.gov/centers/eros/science/usgs-eros-archive-digital-elevation-shuttle-radar-topography-mission-srtm-1">https://www.usgs.gov/centers/eros/science/usgs-eros-archive-digital-elevation-shuttle-radar-topography-mission-srtm-1</a>	2014	30×30	Digital Elevation Model DEM
<a href="https://earthexplorer.usgs.gov/">https://earthexplorer.usgs.gov/</a>	02/18/2023	30×30	Visible From the Landsat OLI 8 Satellite
<a href="https://www.esri.com/en-us/arcgis/about-arcgis/overview">https://www.esri.com/en-us/arcgis/about-arcgis/overview</a>	2014	Process, Display and Analyze Data	Arc GIS 10.8

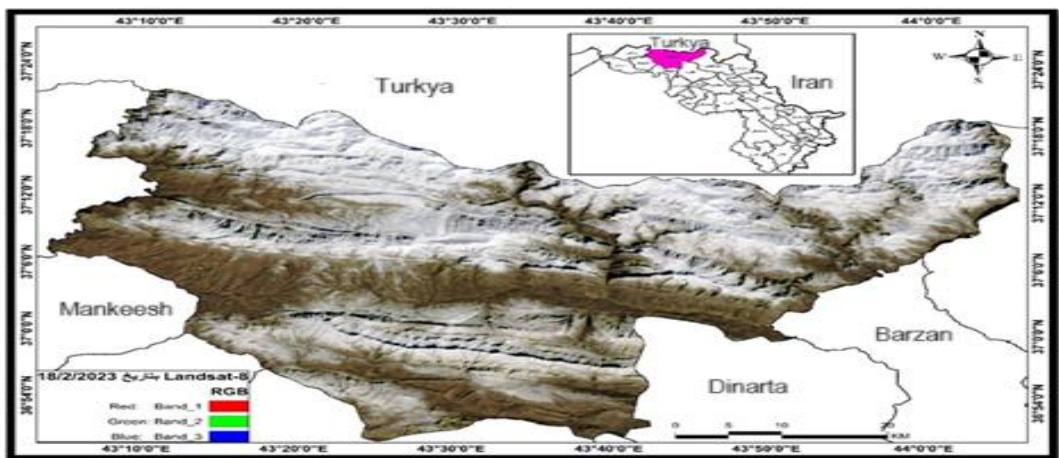


**Figure (1):** Location of the Study Area in Dohuk District.

**Source:** Based on Landsat 8 Data for the Year 2023, Using Arcgis 10.8 Software.

### The Tools and Methods Utilized

Various tools, methods, and software were employed in the research to facilitate the production and completion of the study's requirements, as outlined in Table (1), along with the equations, indicators, and criteria utilized in the study, as illustrated in Table (2).

**Table (2):** Equations, Criteria, and Indicators.

Source	The Key	Equation	Code
• Holko, L., Gorbachova, L., & Kostka, Z.(2011) .	Range 2: Visible	$T_m \text{ Band 2} - T_m \text{ Band5}$	Ndsi
• Laurin, G. V., Francini, S., Penna, D., Zuecco, G., Chirici, G., Berman, E., & Valentini, R.(2022) .	Green, 0.53 – 0.61 $\mu\text{m}$	-----	
• Shnishal, B. S.(2019) .	Band 5: Shortwave Infrared, 1.55–1.75 $\mu\text{m}$	$T_m \text{ Band2} - T_m \text{ Band5}$	

### 3. Remote Sensing Characteristics of Snow Cover

#### 1- Optical and Thermal Properties of Snow Cover

The spectral reflectance of snow depends on numerous factors such as snow crystal size and shape, impurity content, liquid water content near the surface, surface roughness, and solar elevation (Choudhury, 1981, 20, 371-89). Newly fallen snow has remarkably high reflectance in the visible wavelengths (NASA, 1982), as shown in Figure (2). As the snow ages, this reflectance decreases, especially in longer wavelengths (near-infrared), largely due to melting and refreezing within the surface layers, as well as natural impurities. Snow melting leads to an increase in the average size and density of grains by melting smaller particles.

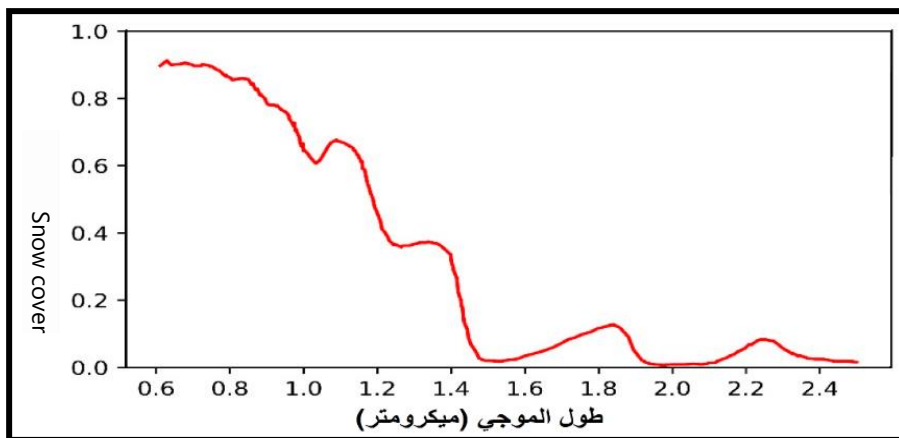


**Figure (2):** Typical Spectral Reflectance Curve of Snow.

**Source:** Choudhury, B.J. And Chang, A. T .C, Two-Stream Theory of Reflectance of Snow . IEEE Trans. Geosci. Electron.1997, GE-17, 63-8.

#### 4. Electrical Properties of Ice and Snow

Remote sensing can be achieved through microwave radiation, either by measuring the emitted radiation using a radiometer, as depicted in Figure (3), or by measuring the intensity of the microwave signal return (in decibels), as with radar. The electrical properties that govern the

material's dielectric constant strongly influence microwave emission and return (Chang, T.e., et al., 1976, pp. 23-39).

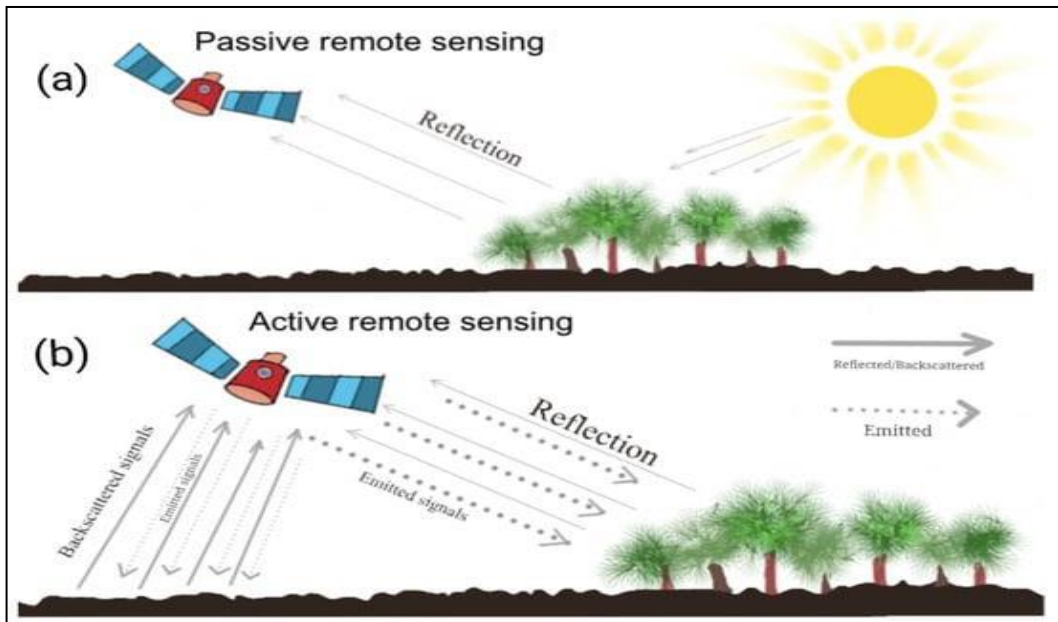


**Figure (3):** Components of the Microwave Signal, Negative and Effective.

**Source:** John Wiley & Sons, Remote Sensing, and Image Interpretation 1979, P52.

## 5. Optical Properties of Snow

The reflection of snow in the visible region of the electromagnetic spectrum depends on the quantity and type of pollutants. Fresh, uncontaminated snow is highly reflective, with reflectance close to unity, regardless of grain size. Conversely, snow with larger grains exhibits less reflectance in the near-infrared region compared to snow with finer grains. This is attributed to light absorption by the larger snow grains relative to the smaller ones. This difference in reflection can be measured empirically, providing a means to determine the effective grain diameter. Consequently, it enables the differentiation of several types of snow, such as high, soft, medium, coarse, very coarse, and extreme snow. The size of snow grains is crucial for determining the reflectance and thickness of the snow cover, as depicted in Figure 4. Optical remote sensing techniques are utilized to monitor various properties of snow, including pollutant concentration, average grain size, and spectral reflectance (Dozier, J. & Painter, T.H., 2004, pp. 465-494). Additionally, the global snow cover extent and its temporal behavior can be studied using remote optical sensing methods (Seidel, K. & Martinec, J., 2004). Generally, fresh snow cover exhibits exceedingly high reflectance in the visible spectrum. However, brightness decreases significantly if the snow is contaminated with pollutants such as dust and algae (Warren, S.G., 1982, pp. 67–89). The decrease in snow brightness due to contamination can be easily detected using a radiometer or a spectrometer operating in the visible to ultraviolet spectral range. Snow reflectance in the visible spectrum is affected by grain size, with ice grains absorbing solar radiation in the near-infrared spectral band. The amount of electromagnetic energy absorbed by the ice grains depends on their size, with larger grains absorbing more energy than smaller ones. Consequently, this reduces light reflection in the

near-infrared spectrum at a wavelength of 1.24 micrometers.

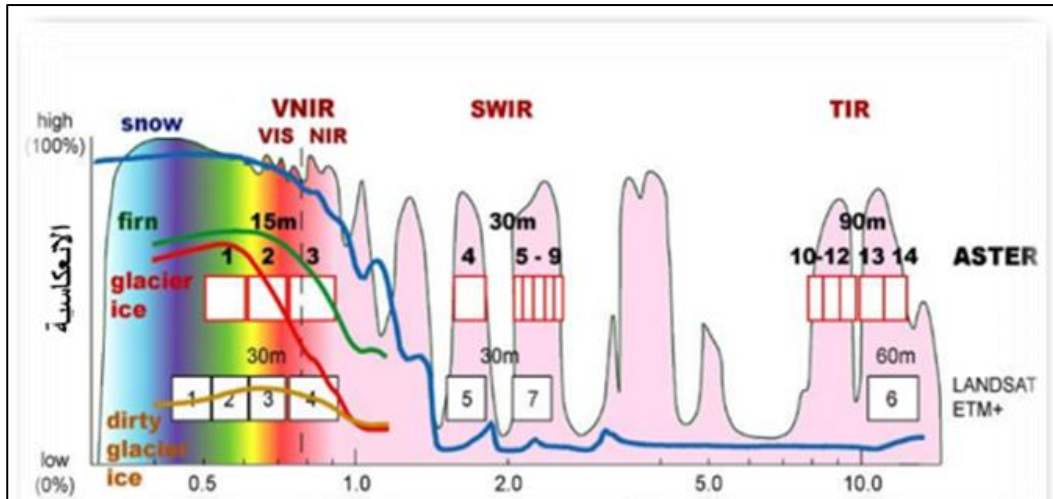


**Figure (4):** Illustrates the Variation in Reflectance Between Snow and Ice.

**Source :** <https://www.bing.com/images/search?view=detailv2&ccid>.

### The Optical Properties of Snow Cover Can be Categorized as Follows

**3-1 Grain Size:** Determining the size of snow grains is crucial as it provides information about the thermal history of the snowpack. The size of dry snow grains affects reflection in the near-infrared spectral region (Dozier, J., 1989, v.28, p15). Satellite imagery can be utilized to estimate grain size, with the most reliable method relying on wavelengths corresponding to the Landsat-OLI or ETM+ sensors in bands 5 and 7, with wavelengths of 1.55 to 1.75 micrometers and 2.08 to 2.35 micrometers, respectively. However, at shorter wavelengths, radiation penetration into the snowpack complicates matters, requiring data correction due to geometric distortions (atmospheric effects, displacement, etc.) (Nolin and Dozier, 2000, p 210).

**3-2 Snow Surface Temperature:** The surface temperature of snow can be derived from thermal infrared measurements within the wavelength range of 10.5 to 12.5 micrometers. The reflectivity of snow is close to unity (Warren, S.G., 1982, p69), making the range of 6 from the Landsat satellite and its equivalents a reliable means for temperature measurement. Atmospheric scattering results in errors of up to approximately 10 Kelvin, but these can be corrected through modeling or calibration using surface data since atmospheric effects do not vary rapidly with location (Orheim and Lucchitta, 1988, p116). Additionally, the dual-view capability of the ERS ATSR instrument allows for direct estimation of atmospheric correction (Bamber, J.L. and Harris, 1994, p21).

**3-3 Radar Properties:** Radar properties refer to the specific characteristics of the snowpack that govern the microwave backscatter coefficient. Several factors influence radar properties. For instance, dry and deep snow leads to scattering of the radar beam, with key variables being grain density and size. Conversely, shallow, dry snow with deep snowpack and contributions from underlying topography are also significant factors. In the case of wet snow, the primary mechanism is scattering on the surface, with key variables including the dielectric constant of the snow (controlled by its density and liquid water content), surface roughness properties, and incident angle. Generally, radar data that measures a single variable (such as backscatter coefficient at a single frequency and polarization) will not be able to separate the effects of

these variables and can only identify ranges of consistent values (Guneriusen, T., et al., 2001, p 2105).

- **Practical Procedures**

- **Platforms and Indicators Used in Monitoring Snow Cover**

(Platforms and sensors used in snow cover monitoring)

In this study, sensors operating across a range from gamma-ray wavelengths to extremely high frequencies (VHF) have been employed in remote sensing studies of snow. While all objects emit radiation across the electromagnetic spectrum, it is beneficial in most studies to utilize data from sensors operating in distinct portions of the spectrum. The user should judiciously select the appropriate sensor for a specific analysis, considering factors such as wavelength, polarization, frequency, and temporal coverage. In general, satellite data from sensors aboard visual and near-infrared satellites, such as those from Landsat and NOAA satellites, are more readily available than other data sources, particularly aerial imagery from aircraft. The frequent coverage provided by satellites like Landsat and NOAA is valuable for many studies. However, sensors operating in the visible and near-infrared wavelengths cannot produce cloud-free images. Thermal infrared data can be acquired at night but not through clouds. Microwave data (both positive and negative) can be obtained day or night and penetrate most cloud cover, but their interpretation is currently more challenging than visible, near infrared, and thermal infrared data due to factors such as surface and subsurface conditions, temperature, surface roughness, and electrical properties.

One of the most important sensors and platforms used in snow cover monitoring is the Operational Land Imager (OLI) carried by the Landsat-8 satellite. OLI is a multispectral radiometric scanner composed of eight bands capable of providing high-resolution imaging data of the Earth's surface. It detects spectrally filtered radiation in the VNIR (Visible-Near Infrared), SWIR (Short-Wave Infrared), LWIR (Long-Wave Infrared), and Panchromatic bands from sunlit Earth over a wide swath width of 183 kilometers at an orbit altitude of 705 kilometers.

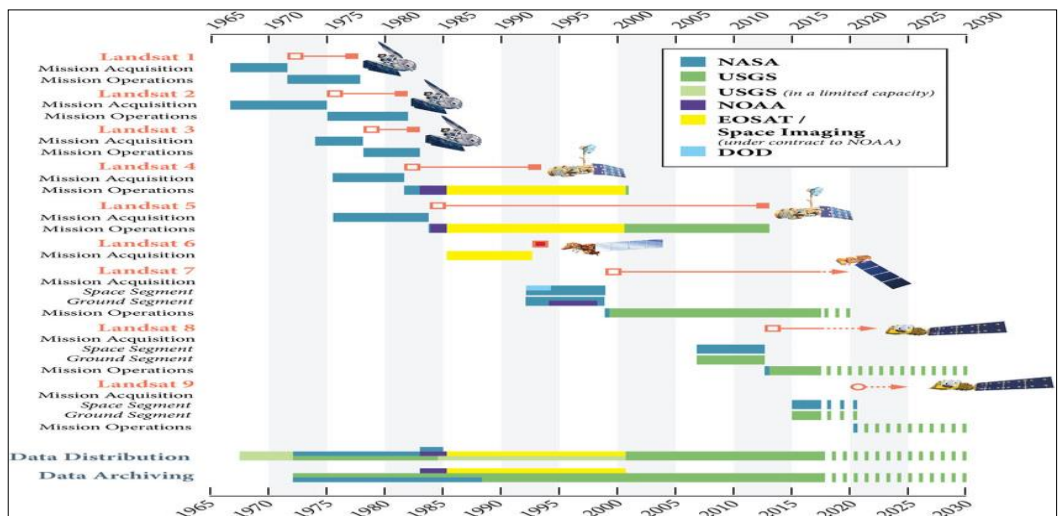


**Figure (5):** Landsat-8 Satellite Characteristics.

Monitoring snow cover extent through the Normalized Difference Snow Index (NDSI)

indicates the relative magnitude of the difference in reflectance between visible (green) and shortwave infrared (SWIR) wavelengths. It controls the contrast between two ranges (one in near infrared or shortwave infrared and the other in the visible parts of the spectrum), which is useful for distinguishing and separating snow, ice, and clouds. Snow is not only highly reflective in the visible parts of the electromagnetic spectrum but also highly absorbing in the near-infrared (NIR) part of the spectrum, while most cloud reflectance remains high in the same parts of the spectrum (Amin, R. A. M. 2019:37-43). This allows for good separation of most clouds and snow (Charlotte Poussin et al, 2023, p21), as shown in Figure 6, which illustrates the extraction of snow cover extent using the NDSI index, and Figure 7, which demonstrates the extraction of snow cover extent using the NDSI index through logical reasoning, and Figure 4 through Python programming language.

**Table (3):** Snow Cover Extent Using the Normalized Difference Snow Index (NDSI).

satellite	Sens or	Equation	Spectral beams		Wavelength
			Band	Green	$\mu\text{m}$
Landsat 8-9	OLI	$(\text{Band 3} - \text{Band 6}) / (\text{Band 3} + \text{Band 6})$	Band 3	Green	Green 0.525–0.600
			Band 6	Short-wave infrared	Short-wave infrared 1.560–1.660

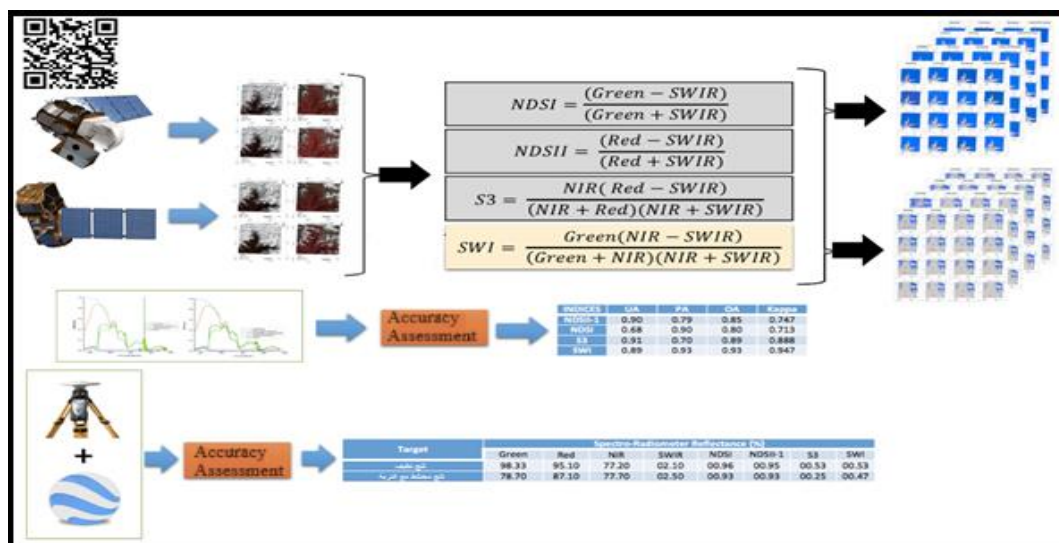


**Figure (6):** Illustrates the Process of Extracting Snow Cover Extent Using the Normalized Difference Snow Index (NDSI).

• **Analysis of the Results**

**Monitoring Snow Cover Using the Normalized Difference Snow Index (NDSI)**

The snow cover changes were monitored and observed using the Operational Land Imager (OLI) mounted on the Landsat-8 satellite, specifically within the spectral bands (Band3, Band6), and leveraging Geographic Information System (GIS) software (Rößler, S., 2021:31).

Scientists have developed methods to continuously monitor and measure the amount of snow covering the land. This data aids in understanding long-term climate variations. Furthermore, it facilitates the assessment of water quantity resulting from snowmelt each winter, its timing, and various associated impacts (Voudouri, K. A., 2023:1569). Visual data from February 18, 2023, was utilized to determine the snow cover area and thickness in the region, which was then segmented based on administrative units.

### 1. Snow Cover Area

Based on the data provided in Table (3) and Figure (7), the snow cover area in the region was approximately 1954.57 km<sup>2</sup>. This area varied across administrative units within the study area. Kani Masî district occupied the first position in terms of area, covering 650.61 km<sup>2</sup>, constituting 33.29% of the total study area. Following it, Shiladze district ranked second with an area of 389.89 km<sup>2</sup>, accounting for 19.95%. In the third position was Dereluk district, covering an area of 337.59 km<sup>2</sup>, representing 17.27% of the total area. Lastly, the smallest area was recorded in the administrative center of the Amadiya district, with a total area of 71.30 km<sup>2</sup>, constituting 3.65% of the total study area.

**Table (4):** Snow Cover Area in the Study Region on (18/02/2023).

Name	Area km <sup>2</sup>	%
Kani Massey	650.61	33.29
Dezi Castle	389.89	19.95
Deira Locke	337.59	17.27
Dhada Manky	260.52	13.33
Saarsink	194.40	9.95
Bamrani	71.30	3.65
Amadiya	50.26	2.57
sum	1957.57	100

**Source:** Based on Data from Map (2).

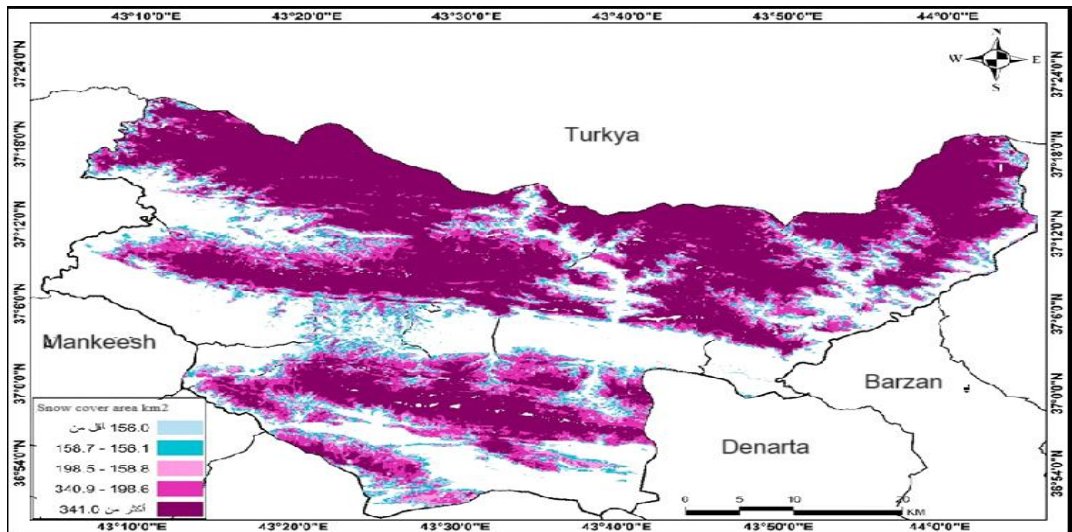


**Figure (7):** Snow Cover Area in Amadiya District on 18/02/2023

**Source:** Landsat 8 Data and ArcMap GIS Software.

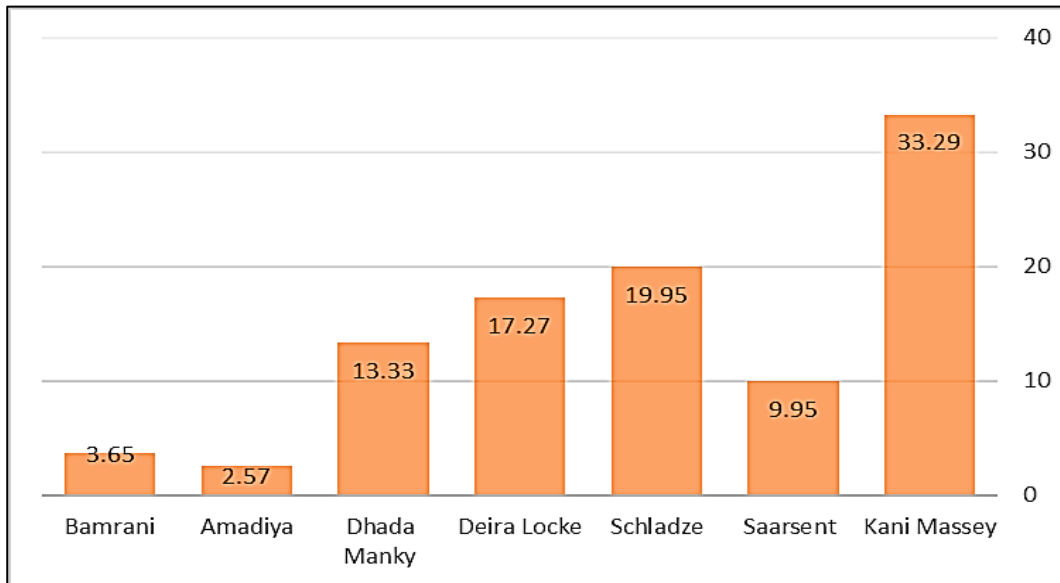
As for the snow cover area within the study area, it appears from the data in Table (4) and



Figure (7) that the Kani Masi district had the highest snow cover area as a percentage of the study area, reaching (86.02%). This was followed by the Sarsink district at (77.47%), then the Sheladize district at (74.89%). The lowest percentage was recorded in the Bamerni district at (29.66%).

**Table (5):** Snow Cover Area as a Percentage of the Study Area.

Snow Cover Area (km <sup>2</sup> )	Administrative Unit Area (km <sup>2</sup> )	Snow Cover Area as Percentage of Study Area (%)	Name
650.61	756.33	33.29	Kani Massey
194.40	250.94	19.95	Saarsent
389.89	520.60	17.27	Schladze
337.59	482.25	13.33	Deira Locke
260.52	436.52	9.95	Dhada Manky
50.26	95.36	3.65	Amadiya
71.30	240.35	2.57	Bamrani
1954.57	2782.35		SUM



**Figure (8):** Percentage of Snow Cover Area Relative to Study Area Area.

**Source:** Based on Table(2)



**Image (1):** Snow Cover in Al-Amadiyah District on 18/02/2023.



**Image (2):** Snow Cover in Amadiya District on 18/02/2023.

## 2- Snow Depth

Snow depth was extracted using the Normalized Difference Snow Index (NDSI). Table (5) illustrates that the study area contained five categories of snow depth. Depth (1) ranked first with an area of 1102.12 km<sup>2</sup>, accounting for 65.34% of the total study area. Following that, the depth range (0.7 - 0.8) centimeters ranked second with an area of 340.87 km<sup>2</sup>, representing 7.42%. Subsequently, the depth range (0.4 - 0.6) centimeters covered an area of 198.51 km<sup>2</sup>, constituting 10.15%. The smallest area was for depths less than 0.04 centimeters, covering 156.02 km<sup>2</sup>, which accounted for 7.98% of the total area, as depicted in Figure (8).

**Table (6):** Snow Depth in Amadiya District on 18/02/2023.

Depth / Meter	Area km2	Ratio %
Less than 0.04	156.02	7.98
0.05 - 0.3	158.74	8.11
0.4 - 0.6	198.51	10.15
0.7 - 0.8	340.87	17.42
More than 1	1102.12	56.34
Total	1956.26	100

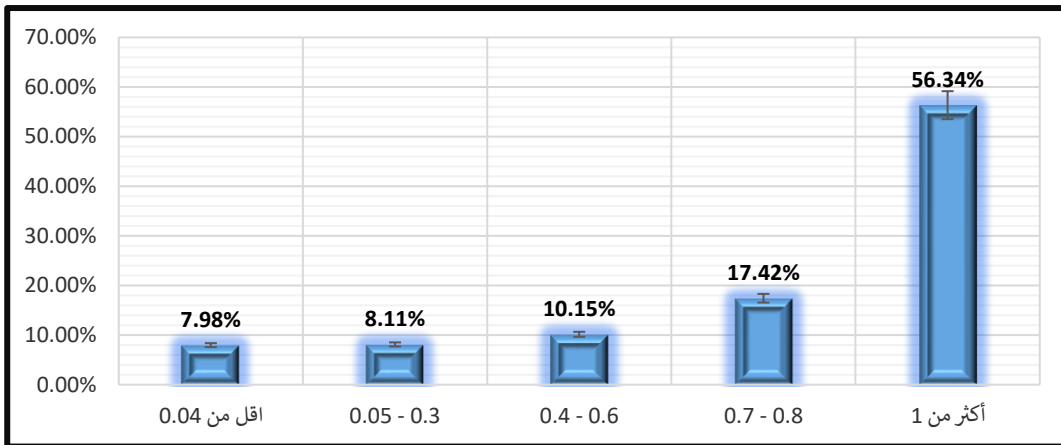


**Figure (9):** Percentage of Snow Depth Based on Area in the Study Area.

**Source:** Derived from the Researcher's Work Based on Table.(3)

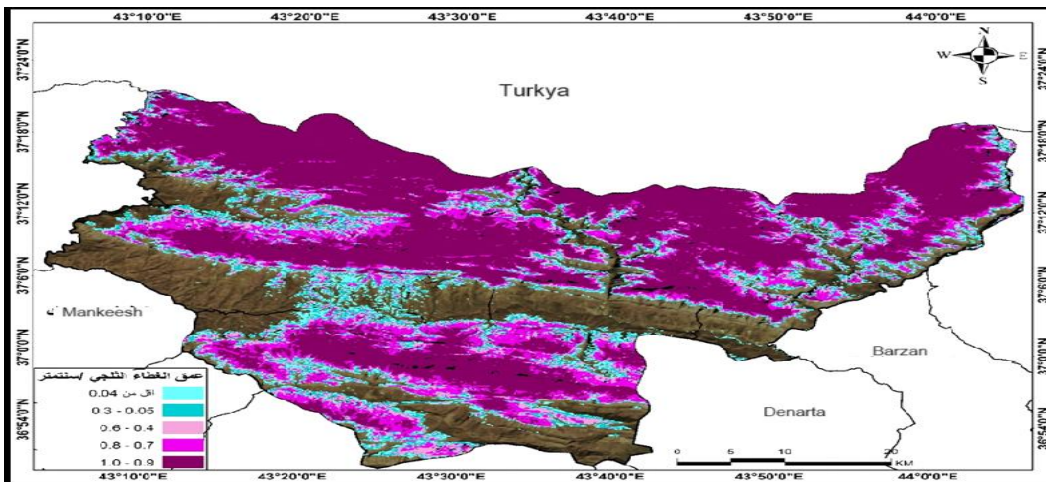


**Figure (10):** Snow Depth in Al-Amadiyah District on February 18, 2023



**Image (3):** Snow Depth of 1 Meter in Al-Amadiyah District at the Serser Border Crossing with Turkey.

The depth of snow based on administrative units in Al-Amadiyah district is illustrated in Table (6). It shows that a depth of one meter occupies the first rank in terms of area in all administrative units. Kani Masi sub-district takes the first place, followed by Sheladzi sub-district, with the Al-Amadiyah district center ranking last. In terms of area, a depth of 0.3 centimeters ranks second, with Kani Masi and Sheladzi sub-districts leading, and the Al-Amadiyah district center ranking last. Meanwhile, a depth of 0.04 centimeters occupies the last position in terms of area.

**Table (6):** Depth of snow cover in administrative units of Al-Amadiyah district on February 18, 2023.

Name	Depth meters	Area / km2	%	Name	Depth meters	Area / km2	%
Dhada Manky	0.04	28.87	11.08%	Bamrani	0.04	11.58	16.24%
	0.3	33.32	12.79%		0.3	9.14	12.82%
	0.6	46.89	18.00%		0.6	9.11	12.77%
	0.8	73.34	28.15%		0.8	13.97	19.60%
	1	78.10	29.98%		1	27.50	38.57%
SUM		260.52	100.00%	SUM		71.30	100.00%
Saarsent	0.04	24.36	12.53%	Kani Massey	0.04	32.61	5.01%
	0.3	21.54	11.08%		0.3	36.75	5.65%
	0.6	22.96	11.81%		0.6	45.47	6.99%
	0.8	35.70	18.36%		0.8	87.74	13.49%
	1	89.84	46.22%		1	448.05	68.87%
SUM		194.40	100.00%	SUM		650.61	100.00%
Aamidi SUM	0.04	6.60	13.12%	Schladze	0.04	29.21	7.49%
	0.3	5.62	11.19%		0.3	28.17	7.23%
	0.6	5.45	10.85%		0.6	36.72	9.42%
	0.8	9.81	19.52%		0.8	61.16	15.69%
	1	22.78	45.32%		1	234.63	60.18%
SUM		50.26	100.00%				
SUM		389.89	100.00%				
Deira Locke	0.04	22.55	6.68%				
	0.3	23.93	7.09%				
	0.6	31.64	9.37%				
	0.8	58.88	17.44%				
	1	200.58	59.42%				
SUM		337.59	100.00%				

## Conclusions

1. Geographic technologies, including Geographic Information Systems (GIS), play a significant role in extracting snow cover areas and snow depth using satellite imagery, such as Landsat-8, and the Snow Cover Index (NDSI).
2. Kani Masi district ranked first in terms of snow cover area within the district, accounting for 33.29% of the total study area. Conversely, the Amadia district ranked last in snow cover area, constituting only 2.57% of the total study area.
3. Regarding the snow cover area as a percentage of the administrative units' area, Kani Masi district had the highest proportion (86.02%), while Bamarne district had the lowest (29.66%).
4. Snow depth of one meter accounted for the largest area within the study area, comprising 56.34% of the total area. Conversely, snow depth of 0.04 centimeters had the smallest area coverage, accounting for 7.98% of the total study area.

## 5. Recommendations

6. The study advocates for further investigations into determining snow coverage in terms of both area and depth using diverse satellite imagery to assess the accuracy of results across different satellites capable of snow cover estimation.
7. Furthermore, the study proposes the establishment of ground monitoring stations to observe snow accumulations in the Al-Amadiyah district, expanding their coverage beyond this district to other regions in northern Iraq.

## References

- Cloudy Skies. *Boundary-Layer Meteorol.* 20, 371-89.
- NASA (1982) Plan of Research for Snowpack Properties Remote Sensing - (PRSI). Recommendations of the Snowpack Properties Research Group, NASA/Goddard Space Flight Center, Greenbelt, MD.
- Choudhury, B.J. and Chang, A. T .C, (1997). Two-stream theory of reflectance of snow .*IEEE Trans. Geosci. Electron.* GE-17, 63-8
- Chang, T.e., Gloersen, P., Schmugge, T, etal, (1976). Microwave emission from snow and glacier ice.*J. Glaciol.* 16, p23-39.
- Dozier, J. & Painter, T.H. (2004). Multispectral and hyperspectral remote sensing of alpine snow properties. *Annual Review of Earth and Planetary Sciences* 32494–465 .
- Seidel, K. & Martinec, J. (2004). *Remote Sensing in Snow Hydrology*. Berlin ,Springer-Praxis.
- Warren, S.G. (1982). Optical properties of snow. *Reviews of Geophysics and Space Physics* 20, 67–89.
- Dozier, J., (1989). Spectral signature of alpine snow cover from the LANDSAT Thematic Mapper. *Remote Sensing of Environment*, v.28, p 15.
- Nolin and Dozier, (2000). A Hyperspectral Method for Remotely Sensing the Grain Size of Snow, *Remote Sensing of Environment*, v 47, p 210.
- Warren, S.G. Optical properties of snow. *Reviews of Geophysics and Space Physics* 20, 1982, p69.
- Orheim and Lucchitta. (1988). Numerical Analysis of Landsat Thematic Mapper Images of Antarctica: Surface Temperatures and Physical Properties, *Annals of Glaciology*, International Glaciological Society, p116.
- Bamber, J.L. and Harris, A.R, (1994). The atmospheric correction for satellite infrared radiometer data in polar regions. *Geophysical Research Letters*, n21, p21.
- Guneriussen, T., Hogda, K. A., Johnsen, H., & Lauknes, I. (2001). InSAR for estimation of changes in snow water equivalent of dry snow. *IEEE Transactions on Geoscience and Remote Sensing*, 39(10), 2101-2108.
- Poussin, C., Timoner, P., Chatenoux, B., Giuliani, G., & Peduzzi, P. (2023). Improved Landsat-based snow cover mapping accuracy using a spatiotemporal NDSI and generalized linear mixed model. *Science of Remote Sensing*, 7, 100078.
- Amin, R. A. M., Al-Asadi, M. A., & Saleh, A. M. (2019). Geo morphotectonic Indicators and Their Impact On The Potential Of The Water Harvesting Using RsGis Al-Baghdadi, Anbar, Iraq Area Study. *Plant Archives*, 19(2), 37-43.
- Rößler, S., Witt, M. S., Ikonen, J., Brown, I. A., & Dietz, A. J. (2021). Remote sensing of snow cover variability and its influence on the runoff of Sápmi's Rivers. *Geosciences*, 11(3), 130.
- Voudouri, K. A., Ntona, M. M., & Kazakis, N. (2023). Snowfall Variation in Eastern Mediterranean Catchments. *Remote Sensing*, 15(6), 1596.

- Holko, L., Gorbachova, L., & Kostka, Z. (2011). Snow hydrology in central Europe. *Geography Compass*, 5(4), 200-218.
- Laurin, G. V., Francini, S., Penna, D., Zuecco, G., Chirici, G., Berman, E., ... & Valentini, R. (2022). SnowWarp: An open science and open data tool for daily monitoring of snow dynamics. *Environmental Modelling & Software*, 156, 105477.
- Shnishil, B. S. (2019). The effect of cloud cover on temperatures in Iraq. *Al-Adab Journal*, (129), 489-506.
- Shnishil, B. S. (2019). Morpho-climatic Modeling by Rain Wrenches and Their Impact on Environmental Degradation Using RS-GIS| Sinjar Mountain Case Study. *Journal of Al-Frahids Arts*, 11.
- Youssef Mohammed Ali Hatem Al-Hathal, & Ahmed Majid Abbas Al-Jubouri. (2019). The Impact of Climate Change on the Variation of the Frequency of Mediterranean and Sudanese Depressions during the Rainy Season in Iraq (A Study in Comprehensive Climatology): The Impact of Climate Change on the Variation of the Frequency of Mediterranean and Sudanese Depressions during the Rainy Season in Iraq (A Study in Comprehensive Climatology). *Medad Al-Adab*, 1(First Part), 37-56.
- Ahmed Majid Abbas & Youssef Mohammed Ali Hatem. (2020). Assessment of Drought in the Jazeera Region in Iraq. *Al-Adab/Al-ādāb*.